Proceedings of CONF-MCEE 2026 Symposium: Advances in Sustainable Aviation and Aerospace Vehicle Automation
DOI: 10.54254/2755-2721/2026.KA28127

Application of Diatomic Electrocatalysts in Oxygen Reduction

Huiyu Liu

College of Chemistry and Chemical Engineering, Nantong University, Nantong, China
2390276303@qq.com

Abstract. Amidst the growing global demand for sustainable energy storage solutions to address energy shortages and environmental concerns, zinc-air batteries (ZABs) have emerged as a promising technology due to their high theoretical energy density and abundance of zinc resources. However, their performance is hindered by the slow kinetics of the oxygen reduction reaction (ORR) at the cathode and the reliance on expensive Pt-based catalysts. This study focuses on the application of a diatomic FeCo-NC electrocatalyst for ORR in ZABs. The catalyst was synthesized using a bimetallic zeolitic imidazolate framework (ZIF-8/ZIF-67) as a precursor via a thermal pyrolysis method. Electrochemical evaluations revealed exceptional ORR activity of the FeCo-NC catalyst in alkaline media, exhibiting a high half-wave potential of 0.875 V and a limiting current density of 5.430 mA cm^{-2}, comparable to commercial Pt/C. Mechanistic studies confirmed a predominant four-electron transfer pathway and favorable reaction kinetics. This work demonstrates the significant potential of atomically dispersed bimetallic catalysts as efficient and cost-effective alternatives to noble-metal catalysts for advanced energy conversion devices like zinc-air batteries, and provides insights into future research directions for precise synthesis and mechanistic understanding.

Keywords: Oxygen reduction reaction, Catalyst, Reaction Kinetics

1. Introduction

Since the 21st century, with the rapid development of society, global energy shortages and environmental pollution have become increasingly severe. The excessive consumption of fossil fuels has exacerbated the energy crisis and led to increased greenhouse gas emissions, further deteriorating the ecological environment [1-4]. With the introduction of China's “carbon peak and carbon neutrality” strategic goals, replacing traditional fossil fuels with clean energy has become an urgent priority. However, renewable energy sources are intermittent and fluctuating, necessitating the development of efficient energy storage technologies [5-8]. Existing lithium-ion batteries, however, face challenges such as resource scarcity and safety concerns, making them unsuitable for grid-scale energy storage needs. Therefore, developing an electrochemical energy storage system that combines high energy density with low cost has become a key objective.

Among various energy storage technologies, zinc-air batteries have garnered significant attention due to their unique advantages. Their theoretical energy density reaches up to 1,353 Wh/kg, approximately five times that of lithium-ion batteries. Zinc resources are abundant, with China's zinc

DOI: 10.54254/2755-2721/2026.KA28127

ore reserves accounting for 20% of the global total and showing a trend of annual growth, exceeding lithium reserves by more than 50 times. Zinc is cost-effective, with zinc battery material costs approximately one-third of those of lithium batteries. Additionally, the byproduct is non-toxic zinc oxide, making it environmentally friendly [9]. Zinc batteries pose no risk of thermal runaway, and their electrolyte is a neutral aqueous solution with a recycling rate exceeding 95%. However, the slow kinetics of the cathode oxygen reduction reaction significantly impair the battery's electrochemical performance [10]. Furthermore, the currently widely used Pt/C catalyst is scarce and expensive, limiting its further commercialization. Therefore, transition metals are being considered as alternatives to precious metal catalysts.

Atomic-level dispersed metal catalysts achieve high activity and stability by highly dispersing metal atoms on the carrier surface. Single-atom catalysts anchor metal atoms on the carrier surface [11-13], achieving 100% atomic utilization, but their active sites are single, prone to agglomeration due to high surface energy, and have symmetrical electronic structures, which inhibit the adsorption and activation of oxygen intermediates. Compared to single-atom catalysts, dual-atom catalysts consist of two adjacent metal atoms, with highly dispersed metal atoms that avoid nanoparticle agglomeration, maximizing active site utilization. Electron transfer between dual-atom sites optimizes reactant adsorption and intermediate formation, stabilizing intermediates and lowering the reaction energy barrier [14-17]. Therefore, we utilize the synergistic effects of bimetallic catalysts to optimize the reaction pathway. We use a high-porosity zeolite imidazolate framework (ZIF) as a precursor and prepare a catalyst with atomically dispersed metal sites through high-temperature pyrolysis [18-24]. This aims to overcome the kinetic bottleneck of the cathode reaction in zinc-air batteries and provide new directions for the design of cathode materials for zinc-air batteries. This research offers a new technical pathway for clean energy storage.

2. Material preparation

2.1. Preparation of ZIF-67

Weigh a certain amount of $Co(NO_3)_2 \cdot 6H_2O$ and dissolve it in 250 mL of methanol. Sonicate for 1 minute to obtain a transparent pink solution with a concentration of 0.04 M. Weigh a certain amount of 2-methylimidazole and dissolve it in 250 mL of methanol. Pour the cobalt nitrate solution into the 2-methylimidazole solution, place it on a magnetic stirrer, and stir for 4 hours. After the reaction is complete, the solution turns into a deep purple suspension. Centrifuge at 8000 rpm for 5 minutes to collect the precipitate. Wash the precipitate three times with methanol and centrifuge to remove unreacted raw materials and solvents. Finally, place the purple precipitate in a vacuum drying oven and dry at 60°C for 12 hours to obtain ZIF-67 powder.

2.2. Preparation of ZIF-8

Weigh a certain amount of $Zn(NO_3)_2 \cdot 6H_2O$ and dissolve it in 250 mL of methanol. Ultrasonicate for 1 min to obtain a transparent pink solution with a concentration of 0.04 M. Weigh a certain amount of 2-methylimidazole and dissolve it in 250 mL of methanol. Pour the cobalt nitrate solution into the 2-methylimidazole solution and stir on a magnetic stirrer for 4 h. After the reaction, the solution turns into a deep purple suspension. Centrifuge at 8000 rpm for 5 minutes to collect the precipitate. Wash the precipitate three times with methanol and centrifuge to remove unreacted raw materials and solvents. Finally, place the purple precipitate in a vacuum drying oven and dry at 60°C for 12 hours to obtain ZIF-8 powder.

DOI: 10.54254/2755-2721/2026.KA28127

2.3. Preparation of the bimetallic catalyst FeCo-NC

Take 0.2 g, 0.4 g, and 0.6 g of ZIF-8 powder, respectively, and add them to the precursor solution for ZIF-67 preparation (i.e., a mixture of cobalt nitrate and 2-methylimidazole) for a 4-hour stirring process. After the reaction, a purple suspension was obtained. The suspension was then centrifuged at 8000 rpm for 5 minutes to collect the precipitate. The precipitate was washed three times with methanol and once with ethanol. The purple precipitate was placed in a vacuum drying oven and dried at 60°C for 12 hours to obtain the ZIF-8/ZIF-67 composite material. The composite material was placed in a tube furnace for carbonization at 900°C. A small amount of $Fe(NO_3)_2 \cdot 6H_2O$ was added to the material after the first carbonization, and it was placed in the tube furnace for a second carbonization, ultimately yielding the target product, the bimetallic catalyst FeCo-NC.

3. Results and discussion

The oxygen reduction reaction (ORR) catalytic performance of the bimetallic catalyst FeCo-NC was systematically evaluated in an alkaline medium using a rotating disk electrode (RDE) setup. As clearly demonstrated in the cyclic voltammetry (CV) profiles presented in Figure 1, no discernible ORR reduction peak was observed when the measurements were conducted under a N_2-saturated atmosphere, confirming the absence of non-faradaic processes or side reactions that could be misinterpreted as ORR activity. In contrast, under an O_2-saturated environment, a well-defined and pronounced cathodic peak emerged, unequivocally indicating the occurrence of the oxygen reduction process. The peak potential was identified at 0.852 V vs. RHE, which notably surpasses the value of 0.837 V documented in the literature for commercial 20% Pt/C catalysts under comparable testing conditions [25]. This positive shift in reduction potential signifies a lower overpotential and more favorable kinetics for the ORR on the FeCo-NC catalyst. The results strongly affirm that FeCo-NC not only facilitates the oxygen reduction reaction in alkaline media but also exhibits exceptional electrocatalytic activity, highlighting its potential as a highly efficient and cost-effective alternative to platinum-based catalysts for applications in advanced energy conversion systems.

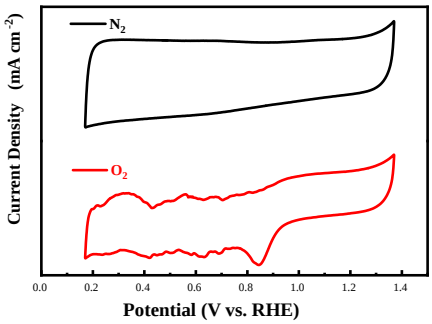

Figure 1. Cyclic voltammetry curve of the diatomic catalyst FeCo-NC

Subsequently, to comprehensively evaluate and compare the electrocatalytic performance toward the oxygen reduction reaction, linear sweep voltammetry (LSV) measurements were conducted on various catalysts using a rotating disk electrode (RDE) at a rotation speed of 1600 rpm, as depicted in Figure 2. The obtained LSV curves revealed significant differences in both the limiting diffusion current density (JL) and the half-wave potential ($E_{1/2}$), which are key indicators of catalytic activity and efficiency. Specifically, the JL values for Co-NC-9, Co-NC-18, Co-NC-36, and FeCo-NC were

DOI: 10.54254/2755-2721/2026.KA28127

determined to be 4.725 mA cm^{-2}, 5.465 mA cm^{-2}, 5.355 mA cm^{-2}, and 5.430 mA cm^{-2}, respectively. Correspondingly, the half-wave potentials for these catalysts were measured at 0.838 V, 0.845 V, 0.848 V, and 0.875 V, respectively.

Among all the samples, the bimetallic FeCo-NC catalyst demonstrated the most promising performance, exhibiting the most positive half-wave potential of 0.875 V, along with a high limiting current density of 5.430 mA cm^{-2}, which is closely comparable to that of benchmark commercial Pt/C catalysts. These results clearly indicate that the ORR electrocatalytic performance of FeCo-NC has approached, and in terms of onset and half-wave potential, even surpassed that of Pt/C. The superior activity can be predominantly ascribed to the strategic introduction of iron, which facilitates the formation of synergistic bimetallic (Fe-Co) sites within the nitrogen-doped carbon matrix. This synergistic interaction not only increases the density and accessibility of active sites but also optimizes the local electronic configuration, thereby enhancing charge transfer kinetics and strengthening the catalyst's capacity for oxygen adsorption and activation.

In contrast, monometallic cobalt-based catalysts (such as the Co-NC series) possess a more uniform and symmetric electronic environment, which tends to hinder effective oxygen binding and subsequent reduction, resulting in comparatively inferior ORR performance. Thus, the integration of iron into the Co-NC structure effectively modulates the catalytic interface, leading to enhanced overall reactivity and durability, and underscoring the importance of bimetallic synergy in the rational design of high-performance non-precious metal catalysts for alkaline fuel cells and related energy technologies.

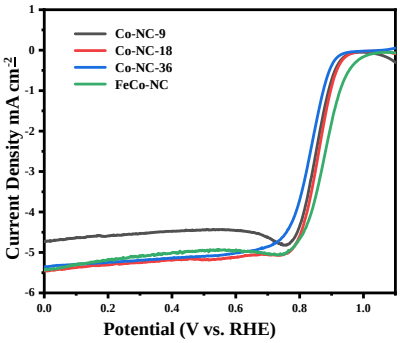

Figure 2. Linear sweep voltammetry curves of ORR for different catalysts

To gain deeper insights into the oxygen reduction reaction kinetics and the underlying electron transfer mechanism of the FeCo-NC catalyst, a series of linear sweep voltammetry (LSV) tests were systematically performed across a range of rotation speeds from 900 to 2500 rpm. It is well-established that increasing the rotation rate enhances the diffusion rate of dissolved O_2 toward the electrode surface, thereby accelerating mass transport and facilitating a more efficient supply of reactant species. As clearly illustrated in Figure 3a, the resulting LSV curves exhibit a pronounced dependence on rotation speed, with the limiting diffusion current density showing a marked increase as the rotation speed is elevated, consistent with improved convective mass transfer under higher hydrodynamic conditions. To quantitatively assess the electron transfer mechanism governing the ORR process, Koutecký-Levich (K-L) analysis was employed based on the LSV data collected at various rotation rates. The K-L plots, constructed at different electrode potentials, demonstrated excellent linearity and parallelism, indicative of first-order reaction kinetics with respect to dissolved oxygen concentration. As presented in Figure 3b, the electron transfer number (n) was

DOI: 10.54254/2755-2721/2026.KA28127

calculated to be approximately 4.0 per oxygen molecule, unequivocally confirming that the ORR on FeCo-NC predominantly proceeds via a highly efficient four-electron transfer pathway. This pathway favors the direct reduction of oxygen to water, as opposed to the two-electron route which results in the formation of intermediate hydrogen peroxide (H_2O_2).The prevalence of the four-electron mechanism not only enhances the overall catalytic efficiency but also significantly mitigates the generation of corrosive peroxide species, thereby reducing the risk of electrode degradation and catalyst instability. Consequently, the FeCo-NC catalyst demonstrates improved durability and operational sustainability, making it a promising candidate for applications in alkaline energy conversion devices such as fuel cells and metal-air batteries [26-27].

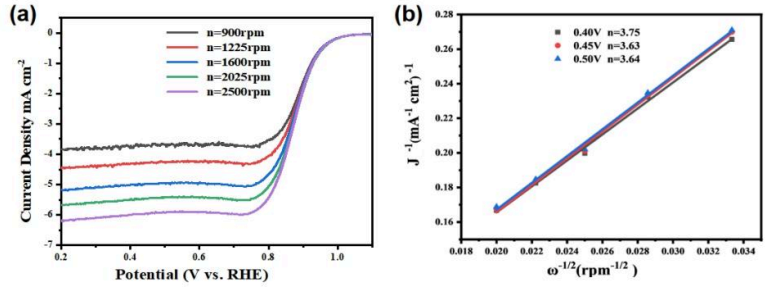

Figure 3. (a) Linear sweep voltammetry test of FeCo-NC in the speed range of 900–2500 rpm (b) Koutecky-Levich (K-L) curve analysis to calculate the number of electron transfers n

To gain further insight into the catalytic kinetics of the oxygen reduction reaction (ORR), Tafel analysis was performed based on the LSV curves obtained at a rotation speed of 1600 rpm for the various catalysts, as summarized in Figure 4. The Tafel slope, a key kinetic parameter derived from the relationship between overpotential and log(current density), provides critical information regarding the rate-determining step and the underlying reaction mechanism. Comparative analysis of the Tafel slopes revealed distinct differences among the catalysts. Specifically, the bimetallic FeCo-NC catalyst exhibited a Tafel slope of 96 mV dec^{-1}, which was notably higher than those of the monometallic Co-NC variants but still lower than that of the commercial Pt/C benchmark.This intermediate value signifies favorable ORR kinetics, suggesting that FeCo-NC possesses a more efficient catalytic interface for oxygen reduction compared to its single-atom counterparts. The enhanced kinetic behavior is attributed to the synergistic interaction between Fe and Co metal sites embedded within the nitrogen-doped carbon matrix, which facilitates improved electronic configuration and promotes more optimal adsorption and desorption of oxygen intermediates. Although the Tafel slope remains slightly elevated relative to Pt/C, the bimetallic catalyst still demonstrates superior kinetic performance over traditional non-noble metal catalysts, enabling accelerated electron transfer and more efficient reactant conversion during the ORR process. The results underscore the effectiveness of the bimetallic design strategy in modulating the electrocatalytic properties and improving overall reaction kinetics, highlighting the potential of FeCo-NC as a durable and highly active catalyst for advanced energy technologies.

DOI: 10.54254/2755-2721/2026.KA28127

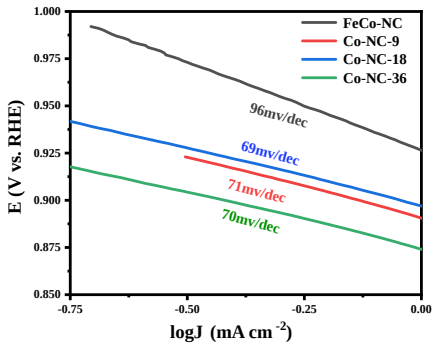

Figure 4. Tafel curves of different catalysts

4. Conclusion and outlook

This study used ZIF-8/ZIF-67 as precursors and employed a solvent-thermal method combined with high-temperature calcination of ZIF to successfully synthesize Co-NC electrocatalysts [28]. Electrochemical testing results indicate that the catalyst exhibits optimal electrocatalytic performance when the zinc-cobalt molar ratio is 18:1. Therefore, based on this precursor, Fe sources were further introduced prior to high-temperature calcination to prepare FeCo-NC bimetallic catalysts. Experimental results show that this bimetallic catalyst exhibits outstanding electrocatalytic activity, with a half-wave potential of 0.875 V, performance comparable to commercial Pt/C catalysts [29], providing an innovative solution to overcome the technical bottlenecks of zinc-air batteries. Additionally, characterization of the material using scanning electron microscopy (SEM) confirmed that the metal active sites in the material are atomically dispersed. This indirectly indicates that metal catalytic efficiency is optimal at the atomic level. Compared to single-atom catalysts, bimetallic catalysts leverage synergistic effects between metal sites to achieve performance comparable to noble metal benchmark materials [30], coupled with significant cost advantages, demonstrating immense application potential in electrochemical reactions and broad industrialization prospects. Based on the above research, we propose the following outlook:

(1) Explore precise synthesis methods. Although various synthesis strategies for bimetallic catalysts have been reported, the structural precision remains challenging to achieve as expected. Given the broad industrial application prospects of bimetallic synergistic effects, future research could leverage artificial intelligence (AI) technology for design assistance to achieve more precise synthesis. For example, computational methods such as density functional theory (DFT) or d-band center theory could be employed to further predict and optimize precise synthesis methods.

(2) Conduct in-depth mechanism studies. Although there has been some research on the reaction mechanisms of bimetallic catalysts in catalytic processes, compared to the relatively well-established research framework for single-atom catalysts, its development remains in its infancy. Currently, our understanding of the intrinsic mechanisms of bimetallic synergistic effects, structure-activity relationships, and complex reaction mechanisms under actual conditions is still limited [31]. Fundamental scientific issues such as bimetallic synergistic mechanisms, coordination environments, and interactions between metals and supports require further in-depth analysis.

(3) Systematically elucidate the “structure-activity” relationship. In addition to the selection of metal combinations, the coordination environment and metal-support interactions also need to be considered. In the future, it is essential to comprehensively consider multiple factors to systematically elucidate the intrinsic connection between structural features and catalytic activity,

DOI: 10.54254/2755-2721/2026.KA28127

further refining reaction mechanism studies. This is crucial for enhancing catalytic performance and is expected to drive breakthrough progress in the application of bimetallic catalysts in the clean energy sector.

References

[1] Zouhri K., Lee S. Y. Evaluation and Optimization of the Alkaline Water Electrolysis Ohmic Polarization: Exergy Study [J]. International Journal of Hydrogen Energy, 2016, 41(18): 7253-7263.

[2] Navarro-Flores E., Chong Z. W., Omanovic S. Characterization of Ni, NiMo, NiW and NiFe Electroactive Coatings as Electrocatalysts for Hydrogen Evolution in an Acidic Medium [J]. Journal of Molecular Catalysis a-Chemical, 2005, 226(2): 179-197.

[3] Wang Z. L., Hu Y. M., Liu W. J., et al. Manganese-Modulated Cobalt-Based Layered Double Hydroxide Grown on Nickel Foam with 1D-2D-3D Heterostructure for Highly Efficient Oxygen Evolution Reaction and Urea Oxidation Reaction [J]. Chemistry-a European Journal, 2020, 26(42): 9382-9388.

[4] Zhai W. F., Chen Y., Liu Y. D., et al. Bimetal-Incorporated Black Phosphorene with Surface Electron Deficiency for Efficient Anti-Reconstruction Water Electrolysis [J]. Advanced Functional Materials, 2023, 33(25): 202301565.

[5] Zhang F. F., Zhang H., Salla M., et al. Decoupled Redox Catalytic Hydrogen Production with a Robust Electrolyte-Borne Electron and Proton Carrier [J]. Journal of the American Chemical Society, 2021, 143(1): 223-231.

[6] Xie H., Feng Y. F., He X. Y., et al. Construction of Nitrogen-Doped Biphasic Transition-Metal Sulfide Nanosheet Electrode for Energy-Efficient Hydrogen Production via Urea Electrolysis [J]. Small, 2023, 19(17): 202207425.

[7] Wang L. P., Zhu Y. J., Wen Y. Z., et al. Regulating the Local Charge Distribution of Ni Active Sites for the Urea Oxidation Reaction [J]. Angewandte Chemie-International Edition, 2021, 60(19): 10577-10582.

[8] Zhang L. S., Wang L. P., Lin H. P., et al. A Lattice-Oxygen-Involved Reaction Pathway to Boost Urea Oxidation [J]. Angewandte Chemie-International Edition, 2019, 58(47): 16820-16825.

[9] Miao R., He J. K., Sahoo S., et al. Reduced Graphene Oxide Supported Nickel-Manganese-Cobalt Spinel Ternary Oxide Nanocomposites and Their Chemically Converted Sulfide Nanocomposites as Efficient Electrocatalysts for Alkaline Water Splitting [J]. American Chemical cs Catalysis, 2017, 7(1): 819-832.

[10] Kulkarni A., Siahrostami S., Patel A., et al. Understanding Catalytic Activity Trends in the Oxygen Reduction Reaction [J]. Chemical Reviews, 2018, 118(5): 2302-2312.

[11] Xie C. L., Niu Z. Q., Kim D., et al. Surface and Interface Control in Nanoparticle Catalysis [J]. Chemical Reviews, 2020, 120(2): 1184-1249.

[12] Skúlason E., Tripkovic V., Björketun M. E., et al. Modeling the Electrochemical Hydrogen Oxidation and Evolution Reactions on the Basis of Density Functional Theory Calculations [J]. Journal of Physical Chemistry C, 2010, 114(42): 18182-18197.

[13] Lv X. S., Wei W., Wang H., et al. Holey Graphitic Carbon Nitride (g-CN) Supported Bifunctional Single Atom Electrocatalysts for Highly Efficient Overall Water Splitting [J]. Applied Catalysis B-Environmental, 2020, 264: 118521.

[14] Sun H. A., Xu X. M., Kim H., et al. Electrochemical Water Splitting: Bridging the Gaps Between Fundamental Research and Industrial Applications [J]. Energy & Environmental Materials, 2023, 6(5): 12441.

[15] Peng O., Shi R., Wang J., et al. Hierarchical Heterostructured Nickle Foam-Supported Co_3O_4 Nanorod Arrays Embellished with Edge-exposed MoS_2 Nanoflakes foe Enhanced Alkaline Hydrogen Evolution Reaction. [J] Materials Today Energy, 2020, 18: 100513.

[16] Zhang Z., Jiang C., Li P., et al. Benchmarking Phases of Ruthenium Dichalcogenides for Electrocatalysis of Hydrogen Evolution: Theoretical and Experimental Insights [J]. Small, 2021, 17(13): 2007333.

[17] Wang C. D., Humayun M., Debecker D. P., et al. Electrocatalytic Water Oxidation with Layered Double Hydroxides Confining Single Atoms [J]. Coordination Chemistry Reviews, 2023, 478: 214973.

[18] Ge J. H., Liu Z. F., Guan M. H., et al. Investigation of the Electrocatalytic Mechanisms of Urea Oxidation Reaction on the Surface of Transition Metal Oxides [J]. Journal of Colloid and Interface Science, 2022, 620: 442-452.

[19] Li J. X., Cui H. Y., Du X. Q., et al. The Controlled Synthesis of Nitrogen and Iron Co-doped Ni_3S_2@NiP_2 Heterostructures for the Oxygen Evolution Reaction and Urea Oxidation Reaction [J]. Dalton Transactions, 2022, 51(6): 2444-2451.

[20] Seh Z. W., Kibsgaard J., Dickens C. F., et al. Combining Theory and Experiment in Electrocatalysis: Insights into Materials Design [J]. Science, 2017, 355(6321): 4998.

[21] Kovac A., Paranos M., Marcius D. Hydrogen in Energy Transition: A Review [J]. International Journal of Hydrogen Energy, 2021, 46(16): 10016-10035.

DOI: 10.54254/2755-2721/2026.KA28127

[22] Furfari S., Clerici A. Green Hydrogen: the Crucial Performance of Electrolysers Fed by Variable and Intermittent Renewable Electricity [J]. European Physical Journal Plus, 2021, 136(5): 509.
[23] Liu L. F. Platinum Group Metal Free Nano-catalysts for Proton Exchange Membrane Water Electrolysis [J]. Current Opinion in Chemical Engineering, 2021, 34: 100743.
[24] Xu J. Y., Amorim I., Li Y., et al. Stable Overall Water Splitting in an Asymmetric Acid/Alkaline Electrolyzer Comprising a Bipolar Membrane Sandwiched by Bifunctional Cobalt-nickel Phosphide Nanowire Electrodes [J]. Carbon Energy, 2020, 2(4): 646-655.
[25] De-Simón-Martín M., Cortés-Nava B. R., Rodríguez-Parra R., et al. The Role of Green Hydrogen in the Energy Transition of the Industry [J]. Dysautonomia Youth Network of America, 2021, 96(2): 200-206.
[26] Vincent I., Bessarabov D. Low Cost Hydrogen Production by Anion Exchange Membrane Electrolysis: A Review [J]. Renewable & Sustainable Energy Reviews, 2018, 81: 1690-1704.
[27] Chi J., Yu H. M. Water Electrolysis Based on Renewable Energy for Hydrogen Production [J]. Chinese Journal of Catalysis, 2018, 39(3): 390-394.
[28] Chen X., Zhang H., Li X. Mechanisms of fullerene and single-walled carbon nanotube composite as the metal-free multifunctional electrocatalyst for the oxygen reduction, oxygen evolution, and hydrogen evolution [J]. Molecular Catalysis, 2021, 502: 111383.
[29] Li R. P., Li Y. Q., Yang P. X., et al. Synergistic interface engineering and structural optimization of non-noble metal telluride-nitride electrocatalysts for sustainably overall seawater electrolysis [J]. Applied Catalysis B-Environmental, 2022, 318: 121834.
[30] Tatarchuk S. W., Choueiri R. M., Mackay A. J., et al. Understanding the Mechanism of Urea Oxidation from First-Principles Calculations [J]. Chemphyschem, 2024, 25(8): 202300889.
[31] Marwat M. A., Humayun M., Afridi M. W., et al. Advanced Catalysts for Photoelectrochemical Water Splitting [J]. American Chemical Society Applied Energy Materials, 2021, 4(11): 12007-12031.